

GREEN NANOCOMPOSITES BASED ON LIGNIN COATED CELLULOSE NANOCRYSTALS AND POLY(LACTIC ACID): CRYSTALLIZATION, MECHANICAL AND THERMAL PROPERTIES

BORŮVKA Martin¹, PRUŠEK Jan¹

¹Technical University of Liberec, Department of Engineering Technology, Liberec, Czech Republic, EU
martin.boruvka@tul.cz

Abstract

The rising concern towards environmental issues and sustainability increasing interest about polymer composites based on renewable and biodegradable resources. The composites, usually referred to as “green”, can find several biomedical and industrial applications. In case of green nanocomposites has filler phase at least one dimension in the nanometer range. The cellulose nanocrystals (CNC) with impressive mechanical properties, annual renewability, abundance, low density and biodegradability make them ideal candidates for the processing of polymer nanocomposites. However, the main barrier in the processing of the nanocomposites based on CNC is their inhomogeneous dispersion and distribution in the non-polar polymer matrix. The strong tendency of CNC to agglomerate, form interconnected networks and additional hydrogen bonds between nanoparticles is in the paper addressed by use of novel hydrophobic lignin coated CNC (L-CNC). In this paper effect of 1, 2 and 3 wt. % loading of L-CNC content on to the properties of the green nanocomposites based on poly (lactic acid) (PLA) matrix was investigated. Nanocomposites prepared by twin screw extrusion and injection moulding were characterized by means of scanning electron microscopy (SEM), differential scanning calorimetry (DSC), thermogravimetric analysis (TGA) and mechanical testing.

Keywords: Cellulose nanocrystals, lignin coating, polylactic acid, green nanocomposites

1. INTRODUCTION

The polymer composites market share continuously growing. However, based on two different components, recycling and reusing of such composites is quite difficult [1]. During last few decades European regulations pushes towards more sustainable, cost efficient and environmentally friendlier materials and applications [2]. Green composites based on sustainable, biodegradable and renewable resources are of great interest as replacement of petroleum-based polymers and synthetic fillers [3]. This shift will be challenging for automotive industry and will occur only when cost effective and competitive production to conventional injection molded thermoplastics will be achieved [2]. The task in other typical applicative fields like secondary and tertiary structures, panels, packaging and cases that do not require excellent mechanical properties can be made easier [1]. Poly (lactic acid) (PLA) as a biobased, biodegradable and biocompatible thermoplastic with high strength (50-70 MPa) and modulus (3 GPa) still faces important industrial problems such as a slow crystallization, inherent brittleness and low impact resistance to compete with synthetic commodity polymers [3]. Fillers in case of green composites mostly consist of plant fibers that are reinforced by helically arranged semi-crystalline microfibrils of cellulose. Each microfibril is a string of cellulose crystallites, linked along the chain axis by amorphous domains [4]. These crystallites are called cellulose nanocrystals (CNC) and are essential reinforcing element that nature synthesizes to strengthen all the supporting structures of trees, plants and algae's. The CNC are longitudinally released by selective hydrolysis of amorphous domains with typical dimensions ranging from 3-5 nm in width and 50-500 nm in length [5]. Due to almost perfect crystal structure can elastic modulus of individual CNC reach 143 GPa [6]. Coupled with unique characteristics like low density (~ 1.6 g/cm³), high tensile strength (~ 7.5 GPa), low thermal expansion coefficient (~ 1 ppm/K), thermal stability up to ~ 300 °C and high aspect ratio (10-100) [5] could serve as new plant based reinforcing element for future generation of "green" nanocomposites [7]. However, there is main barrier that is needed to be overcome to

avoid inhomogeneous dispersion and distribution of CNC within a non-polar polymeric matrix. The omnipresence of interacting surface hydroxyl groups causing strong tendency of CNC for self-association during nanocomposite processing. Poor dispersion and distribution than limit the potential of mechanical reinforcement and nucleation density capabilities [8]. In this paper is this problem addressed by use of CNC modified with hydrophobic lignin coating (L-CNC) developed by American Process Inc. (API) (USA). The API's low cost hydrophobic coating method is based on precipitation of dissolved lignin from biomass during pretreatment step onto the CNC surface and through the process is physically adsorbed on a surface and then spray dried [5].

2. EXPERIMENTAL

Poly(lactic acid) (PLA) grade Ingeo™ 3251D was purchased from Nature Works LLC (USA). Spray dried powdered lignin coated cellulose nanocrystals (L-CNC) under trade mark BioPlus-L™ Crystals was purchased from American Process Inc. (USA). Before the processing was PLA dried in Maguire Low Pressure Dryer (LPD 100) under the following conditions: temperature 80°C, time 180 min., vacuum 0.8 bar. Nanocomposite pellets and control PLA samples were prepared by twin screw extruder (ZAMAK EHP-2x130di) followed by water bath and pelletizer. Temperature profile of extrusion line was set from 140 °C up to 180 °C. L-CNC was dosed directly into the melting chamber of extruder in the recommended front position by external device, working on the gravimetric principle. The reason for dosing in the front parts of the extruder is to prevent excessive shear stress of L-CNC during melt compounding and thus their damage or thermal degradation. Pelletized compounds passed through a water bath and thus were before injection molding dried at Maguire Low Pressure Dryer (LPD 100) under following conditions: temperature 80°C, time 180 min., vacuum 0.8 bar. Testing specimens were injection molded according to ISO 527 on injection molding machine (ARBURG 270S 400-100) with increasing temperature profile (165 °C up to 190 °C) of the melting chamber. Resulted green nanocomposites and control samples are depicted in **Table 1**. The scanning electron microscope (SEM) examination of L-CNC has been conducted on Carl Zeiss ULTRA Plus (**Figure 3**). One droplet of distill water diluted and ultrasonicated L-CNC powder was placed on carbon tape stage and let dry in a laboratory oven overnight. The dried sample was then gold sputtered with a coating thickness in the order of 1nm. Study of crystallization was conducted by differential scanning calorimetry (DSC) Mettler Toledo DSC 1/700 calorimeter according to ISO 11357. The samples amount 10±1 mg were sealed in an aluminum pan and heated to 200 °C to remove previous thermal history and then cooled again. The second heating-cooling cycle analysis run at 10 °C min⁻¹ heating/cooling ramp in a nitrogen atmosphere (flow rate 50 ml·min⁻¹) to determine thermal transitions: glass transition (T_g), cold crystallization (T_{cc1} and T_{cc2}) and melting (T_m) temperatures and enthalpies (ΔH_{cc1} , ΔH_{cc2} , ΔH_m). The crystalline fraction χ_c (%) of PLA and PLA/L-CNC nanocomposite samples was calculated based on the enthalpy value of a 100 % crystalline PLA from the following equation [9]:

$$\chi_c(\%) = \frac{\Delta H_f - \Delta H_{cc}}{\Delta H_f^0 \cdot W_m} \times 100 \quad (1)$$

where ΔH_f is enthalpy of fusion and ΔH_{cc} is enthalpy of cold crystallization, both determined by DSC. ΔH_f^0 is melting enthalpy of totally crystallized PLA sample ($\Delta H_f^0 = 93 \text{ J} \cdot \text{g}^{-1}$) [4] and W_m is PLA matrix weight fraction in the green nanocomposite sample. Thermal degradation behavior was studied by means of thermal gravimetric analysis (TGA) on a TGA Q500 (TA Instruments, USA). Samples were heated from room temperature to

Table 1 PLA control and green nanocomposite samples

sample code	composition (wt.%)	
	PLA	L-CNC
PLA	100	-
PLA/1-L-CNC	99	1
PLA/2-L-CNC	98	2
PLA/3-L-CNC	97	3

500 °C at a heating ramp 10 °C·min⁻¹ in N₂ atmosphere. The mechanical properties were measured according to international standards (ISO 527, ISO 179-1/1eU, ISO 178). Testing machines for measuring mechanical properties were used as follow: Tensile - TIRAtest 2300, Impact - CEAST Resil 5.5 and Flexural - Hounsfield H10KT.

3. RESULTS AND DISCUSSION

Differential scanning calorimetry was used to investigate the effect of L-CNC content on the glass transition, non-isothermal crystallization and melting phenomena of PLA/L-CNC nanocomposites. Resulted DSC thermograms during second heating are shown in **Figure 1** and thermal properties are summarized in **Table 2**. During heating of the injected parts from PLA and PLA/L-CNC nanocomposites was observed the glass transition temperature T_g , the primary peak cold crystallization temperature T_{cc1} and further the secondary peak cold crystallization T_{cc2} . ΔH_{cc} is exothermic enthalpy that is absorbed by crystals growth during heating. Such cold crystallization of material is related to rapid cooling of the melt in the mould cavity during the injection molding. It negatively influenced not only the structure change and material properties but also shape and dimensional instabilities of injected parts. With increasing content (1, 2 and 3 wt. %) of L-CNC, increased nucleation density and higher crystallization rates of PLA has been enhanced. At the virgin PLA during cooling rate 10 °C·min⁻¹ was not observed sharply defined phase transformation associated to melt crystallization (ΔH_c) of polymer, in contrast to PLA/L-CNC nanocomposites. It was proved that addition of L-CNC to PLA matrix increases the melt crystallization enthalpy (ΔH_c) and decreases the cold crystallization enthalpy ΔH_{cc1} and ΔH_{cc2} as can be seen in **Table 2**. The degree of crystallinity (χ_c) of virgin PLA and green nanocomposites increased from 5.6 % (virgin PLA) to 8.5 % (PLA/1-L-CNC), 10.3 % (PLA/2-L-CNC) and 10.7 % (PLA/3-L-CNC). This corresponds to decrease of specific heat capacity (ΔC_p) in area of glass transitions, related to increase of L-CNC content.

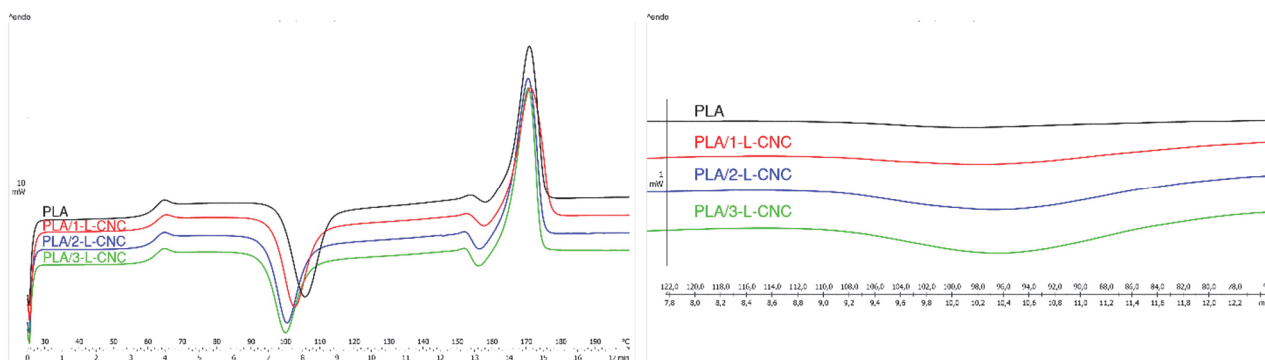


Figure 1 DSC heating (left) and cooling (right) thermograms of PLA and PLA/L-CNC nanocomposites

Table 2 Thermal properties from DSC analysis of PLA and PLA/L-CNC nanocomposites

	ΔC_p [J·g ⁻¹ ·K ⁻¹]	T_m [°C]	ΔH_f [J·g ⁻¹]	ΔH_{cc1} [J·g ⁻¹]	ΔH_{cc2} [J·g ⁻¹]	ΔH_c [J·g ⁻¹]	χ_c (%)
PLA	0.49	170.1	37.9	31.8	0.9	0.3	5.6
PLA/1-L-CNC	0.47	170.6	38.9	29.0	2.1	0.8	8.5
PLA/2-L-CNC	0.45	169.8	41.0	28.7	3.0	1.6	10.3
PLA/3-L-CNC	0.43	169.8	39.7	26.9	3.1	1.9	10.7

Thermogravimetric analysis in N₂ atmosphere was carried out at a heating rate of 10 °C·min⁻¹. Resulted thermal degradation behaviors of PLA and PLA/L-CNC nanocomposites are shown in **Figure 2** and characteristic temperatures of thermal degradation are summarized in **Table 3**. **Figure 3** shows thermogravimetric (left) and weight loss rates (right). Degradation of control α -Cellulose sample started at 303 °C that is related to the first 5 wt. % weight loss of material and reached maximum weight loss rate at 361 °C. Thermal degradation of L-CNC begins at 287 °C and reached maximum weight loss rate at 356 °C. This could be related to lignin molecular structure that is composed mostly of aromatic rings having various branching, these chemical bonds lead to a wide degradation temperatures. Resulted PLA/L-CNC nanocomposites with low L-CNC content exhibit no significant improvement in thermal parameters compared to virgin PLA.

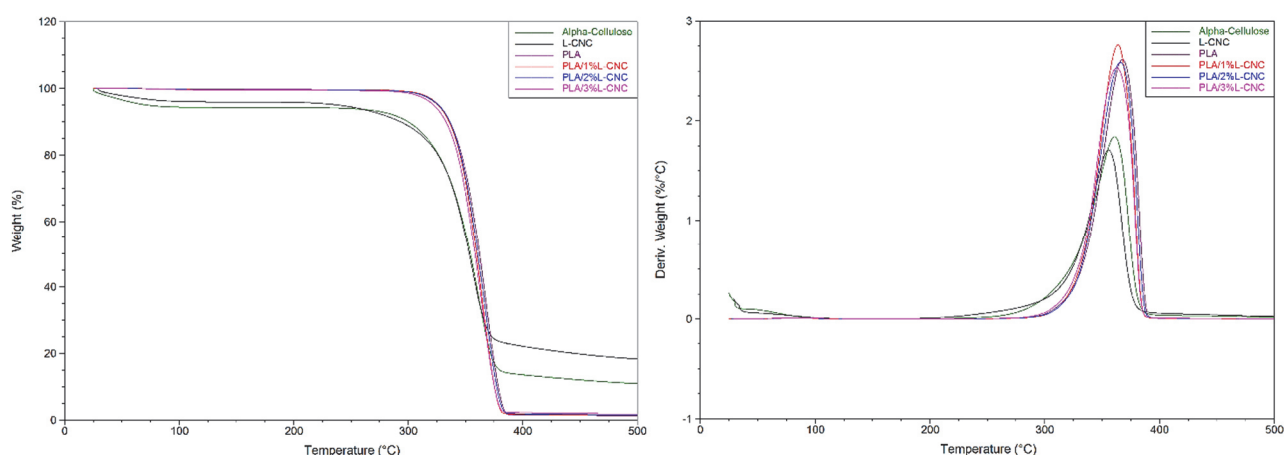


Figure 2 Thermogravimetric traces (left) and weight loss rates (right) of PLA, α -Cellulose, L-CNC and PLA/L-CNC nanocomposites

Table 3 Thermodegradation temperatures and maximum degradation rates of PLA, α -Cellulose, L-CNC and PLA/L-CNC nanocomposites

	α -Cellulose	L-CNC	PLA	PLA/1-L-CNC	PLA/2-L-CNC	PLA/3-L-CNC
$T_{5\%}$ [°C]	303	287	326	327	327	322
T_{peak} [°C]	361	356	368	364	366	364
α_{max} [%/°C]	1.85	1.71	2.61	2.76	2.59	2.53

The mechanical properties are summarized in **Table 4**. Tensile modulus was continuously increased upon increasing L-CNC loading. However, the highest obtained value resulted in only 5 % improvement at highest L-CNC loading (PLA/3-L-CNC). Tensile strength compared to virgin PLA did not show any improvements and decreased with increasing L-CNC content. Both of these problems could be related to insufficient mechanical energy addition to separate the spray-dried L-CNC bundles (**Figure 3**) due to dosing in front position of extruder. The PLA/L-CNC samples are actually composed of both micro L-CNC bundles and individual L-CNCs. Slight improvement in tensile modulus could be related to increased degree of crystallinity (see **Table 2**). The elongation at break of PLA/L-CNC samples as expected decreases with increasing L-CNC content. L-CNC caused local stress concentrations and failure at reduced strain. The impact strength of PLA/L-CNC samples was improved compared to virgin PLA. The addition of only 1 wt.% of L-CNC resulted in increased impact strength by 25%. However, with increasing content of L-CNC impact strength started to decrease. The insufficient distribution and dispersion of L-CNC in PLA matrix limit potential of mechanical reinforcement.

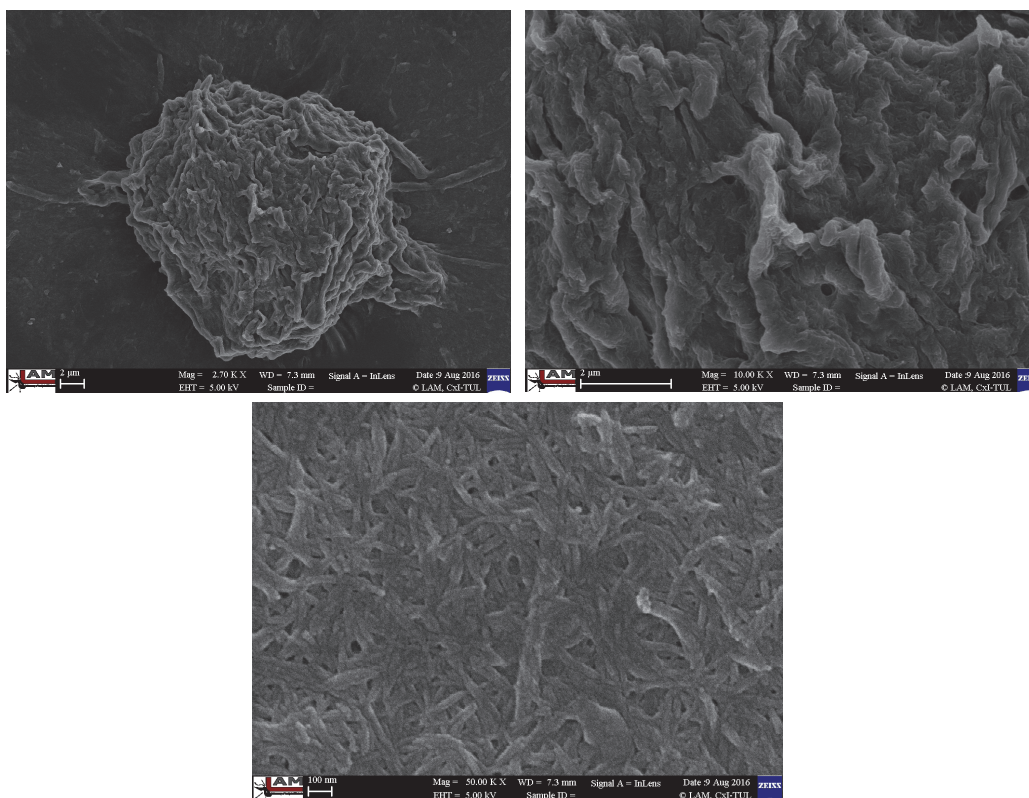


Figure 3 SEM image of spray-dried L-CNC bundle (left), magnified bundle surface (middle) and individual agglomerated L-CNCs forming bundle surface (left)

Table 4 Mechanical properties of PLA and PLA/L-CNC nanocomposites

Mech. properties	Standart	Unit	PLA	PLA/1-L-CNC	PLA/2-L-CNC	PLA/3-L-CNC
Tensile Modulus of Elasticity (1 mm/min)	ISO 527/1B/1	MPa	3882 ± 44	3940 ± 68	4003 ± 79	4071 ± 87
Yield Strength (Ultimate Strength) (50 mm/min)	ISO 527/1B/50	MPa	71.5 ± 0.5	68.9 ± 0.8	67.2 ± 1.7	65.9 ± 2.2
Nominal Strain at Fracture (50 mm/min)	ISO 527/1B/50	%	4.9 ± 0.5	4.7 ± 1.5	4.0 ± 2.1	3.3 ± 2.7
Charpy Impact Energy (+23°C)	ISO 179-1/1eA	kJ/m ²	16.6 ± 0.4	20.7 ± 1.2	18.3 ± 1.7	17.1 ± 2.2

4. CONCLUSION

Lignin coated cellulose nanocrystals were incorporated in poly (lactic acid) biopolymer matrix to investigate influence of surface modification on green nanocomposite properties. The resulted L-CNC/PLA nanocomposites prepared by twin screw extrusion and injection moulding were characterized by means of scanning electron microscopy (SEM), differential scanning calorimetry (DSC), thermogravimetric analysis (TGA) and mechanical testing the effect of L-CNC content on nucleation density and higher crystallization rate of PLA has been observed by DSC. The addition of L-CNC into PLA increased melt crystallization enthalpy and decreased the cold crystallization enthalpy. The degree of crystallinity (χ_c) increased from 5.6 % (virgin PLA) to 8.5 % (PLA/1-L-CNC), 10.3 % (PLA/2-L-CNC) and 10.7 % (PLA/3-L-CNC). Thermal degradation behaviors indicated good thermal stability during processing of PLA/L-CNC nanocomposites. However, the

first 5 wt.% loss of material observed for L-CNC samples started earlier compared to control α -Cellulose samples. This could be related to lignin coating molecular structure that is composed mostly of aromatic rings having various branching, these chemical bonds lead to wide range of degradation temperatures (100 - 800 °C) [11]. Tensile modulus was slightly increased with increasing L-CNC content, while tensile strength decreased with incorporation of L-CNC. The elongation at break of PLA/L-CNC samples as expected decreases with increasing L-CNC content. The impact strength of PLA/L-CNC samples was improved compared to virgin PLA. The addition of only 1 wt.% of L-CNC resulted in increased impact strength by 25%. However, with further increasing content of L-CNC impact strength started to decrease. The low distribution and dispersion of L-CNC in PLA matrix limit potential of mechanical reinforcement. These problems could be related to insufficient mechanical energy addition to separate the spray-dried L-CNC bundles due to dosing in front position of extruder.

ACKNOWLEDGEMENTS

This paper was written with research project SGS 21122 support.

REFERENCES

- [1] F. P. LA MANTIA and M. MORREALE, Green composites: A brief review, *Compos. Part Appl. Sci. Manuf.*, vol. 42, no. 6, pp. 579-588, 2011.
- [2] G. KORONIS, A. SILVA, AND M. FONTUL, Green composites: A review of adequate materials for automotive applications, *Compos. Part B Eng.*, vol. 44, no. 1, pp. 120-127, 2013.
- [3] A. PEI, Q. ZHOU, AND L. A. BERGLUND, Functionalized cellulose nanocrystals as biobased nucleation agents in poly(l-lactide) (PLLA) - Crystallization and mechanical property effects, *Compos. Sci. Technol.*, vol. 70, no. 5, pp. 815-821, 2010.
- [4] A. K. MOHANTY, M. MISRA, AND L. T. DRZAL, *Natural fibers, biopolymers, and biocomposites*. CRC Press, 2005.
- [5] K. NELSON, T. RETSINA, M. IAKOVLEV, A. VAN HEININGEN, Y. DENG, J. A. SHATKIN, and A. MULYADI, American Process: Production of Low Cost Nanocellulose for Renewable, Advanced Materials Applications, in *Materials Research for Manufacturing*, Springer, pp. 267-302, 2016.
- [6] A. ŠTURCOVÁ, G. R. DAVIES, AND S. J. EICHHORN, Elastic Modulus and Stress-Transfer Properties of Tunicate Cellulose Whiskers, *Biomacromolecules*, vol. 6, no. 2, pp. 1055-1061, 2005.
- [7] R. J. MOON, A. MARTINI, J. NAIRN, J. SIMONSEN, and J. YOUNGBLOOD, Cellulose nanomaterials review: structure, properties and nanocomposites, *Chem. Soc. Rev.*, vol. 40, no. 7, pp. 3941-3994, 2011.
- [8] A. DUFRESNE, Nanocellulose: a new ageless bionanomaterial, *Mater. Today*, vol. 16, no. 6, pp. 220-227, 2013.
- [9] E. LIZUNDIA, J. L. VILAS, AND L. M. LEÓN, Crystallization, structural relaxation and thermal degradation in Poly(l-lactide)/cellulose nanocrystal renewable nanocomposites, *Carbohydr. Polym.*, vol. 123, pp. 256-265, 2015.
- [10] LIZUNDIA, ERLANTZ, et al. PLLA-grafted cellulose nanocrystals: Role of the CNC content and grafting on the PLA bionanocomposite film properties. *Carbohydrate polymers*, vol. 142, pp. 105-113, 2016.
- [11] D. WATKINS, M. NURUDDIN, M. HOSUR, A. TCHERBI-NARTEH, and S. JEELANI, Extraction and characterization of lignin from different biomass resources, *J. Mater. Res. Technol.*, vol. 4, no. 1, pp. 26-32, 2015.